Inorg. Chem. **2006**, *45*, 4544–4555

Probing the Electronic Structure of Platinum(II) Chromophores: Crystal Structures, NMR Structures, and Photophysical Properties of Six New Bis- and Di- Phenolate/Thiolate Pt(II)Diimine Chromophores

Julia A. Weinstein,*[,†,‡,§] Mark T. Tierney,[£,+] E. Stephen Davies,[§] Karel Base,[£,¶] Anthony A. Robeiro,[||] and Mark W. Grinstaff*[,#]

Department of Chemistry, The University of Sheffield, Sheffield S3 7HF, United Kingdom, Department of Chemistry, Moscow Lomonosov State University, 119899, Moscow, Russia, School of Chemistry, University of Nottingham, Nottingham NG7 2RD, United Kingdom, Duke University, Durham, North Carolina 27708, Duke NMR Spectroscopy Center and Department of Radiology, Duke University, Durham, North Carolina 27708, and Departments of Chemistry and Biomedical Engineering, Metcalf Center for Science and Engineering, Boston University, Boston, Massachusetts 02215

Received October 6, 2005

A general route for synthesis of six structurally similar Pt(II) diimine thiolate/phenolates chromophores possessing bulky phenolate or thiolate ligands is reported. The Pt chromophores were characterized using an array of techniques including ^{1}H, ^{13}C, and ^{195}Pt NMR, absorption, emission, (spectro)electrochemistry, and EPR spectroscopy. Systematic variation of the electronic structure of the Pt(II) chromophores studied was achieved by (**i**) changing solvent polarity; (**ii**) substituting oxygen for sulfur in the donor ligand; (**iii**) alternating donor ligands from *bis*- to *di*-coordination; and (**iv**) changing the electron donating/withdrawing properties of the ligand(s). The lowest excited state in these new chromophores was assigned to a [charge-transfer-to-diimine] transition from the HOMO of mixed Pt/S (or Pt/O) character on the basis of absorption and emission spectroscopy, UV/vis (spectro)electrochemistry, and EPR spectroscopy. One of the chromophores, Pt(dpphen)(3,5-di-*tert*-butyl-catecholate) represents an example of a Pt-(II) diimine phenolate chromophore that possesses a reversible oxidation centered predominantly on the donor ligand. Results from EPR spectroscopy indicate participation of the Pt(II) orbitals in the HOMO. There is a dramatic difference in the photophysical properties of carborane complexes compared to other mixed-ligand Pt(II) compounds, which includes room-temperature emission and photostability. The charge-transfer character of the lowest excited state in this series of chromophores is maintained throughout. Moreover, the absorption and emission energies and the redox properties of the excited state can be significantly tuned.

Introduction

New transition metal diimine complexes are actively pursued as potential photocatalysts, artificial photosynthetic receptors, photoluminescent nucleic acid probes, and molecular photonic devices.[1−37] Previous reports in this area had concentrated primarily on d^6 diimine complexes, with Ru(bpy)$_3^{2+}$ and its derivatives being the most commonly studied.[5,9−11] The observation by McMillin[12] and Eisenberg[13]

* To whom correspondence should be addressed. E-mail: mgrin@bu.edu (M.W.G.); Julia.Weinstein@sheffield.ac.uk (J.A.W.).
† The University of Sheffield.
‡ Moscow Lomonosov State University.
§ University of Nottingham.
£ Duke University.
|| Duke NMR Spectroscopy Center and Department of Radiology, Duke University.
Boston University.
+ Present address: Ohio University. Department of Chemistry and Biochemistry, Athens, OH 45701.
¶ Present address: Duke University Medical Center, Department of Radiology, Durham, NC 27710.

(1) Cummings, S. D.; Eisenberg, R. *J. Am. Chem. Soc.* **1996**, *118*, 1949.
(2) Weinstein, J. A.; Blake, A. J.; Davies, E. S.; Davis, A. L.; George, M. W.; Grills, D. C.; Lileev, I. V.; Maksimov, A. M.; Matousek, P.; Mel′nikov, M. Y.; Parker, A. W.; Platonov, V. E.; Towrie, M.; Wilson, C.; Zheligovskaya, N. N. *Inorg. Chem.* **2003**, *42*, 7077.
(3) Harriman, A.; Ziessel, R. *Chem. Commun.* **1996**, 1707.
(4) Gray, H. B.; Winkler, J. R. *Annu. Rev. Biochem.* **1996**, *65*, 537.
(5) Juris, A.; Balzani, V.; Barigelletti, F.; Campagna, S.; Belser, P.; von Zelewsky, A. *Coord. Chem. Rev.* **1988**, *84*, 85.
(6) Meyer, T. J. *Acc. Chem. Res.* **1989**, *22*, 163.
(7) Pelizzetti, E.; Serpone, N. Eds.; D. Reidel Publishing: Dordrecht, 1985.
(8) Prasad, P. N.; Williams, D. J. *Introduction to Nonlinear Optical Effects in Molecules and Polymers*; Wiley-Interscience: New York, 1991.
(9) Balzani, V.; Juris, A.; Venturi, M.; Campagna, S.; Serroni, S. *Chem. Rev.* **1996**, *96*, 759.
(10) Sauvage, J. P.; Collin, J. P.; Chambron, J. C.; Guillerez, S.; Coudret, C.; Balzani, V. *Chem. Rev.* **1994**, *94*, 993.

10.1021/ic051733t CCC: $33.50
Published on Web 05/06/2006

of fluid-solution photoluminescence from Cu(I) bis-diimines and Pt(II) diimine dithiolates has led to an interest in tuning and optimizing the electronic structure and photophysical properties of Cu(I) and Pt(II) complexes for specific applications.[1,13−25] Coordinately unsaturated, photoluminescent d^8 metal chromophores, unlike their d^6 counterparts, possess open coordination sites for subsequent chemical reactions such as self-quenching and cross-quenching,[15,26−29] photoreactivity,[30] and photocatalysis.[31] Pt(II) chromophores have also been explored as tunable materials for nonlinear optical,[32,33] light-emitting diode,[34] and solar cells[35] applications, as well as for sensitization of singlet oxygen.[26,36,37]

However, mixed-ligand complexes of Pt(II) with diimine or triimine ligands are often nonemissive in solution at room temperature, largely due to the presence of a population of metal-centered (d−d) states close in energy, which leads to efficient nonradiative deactivation. In recent years, two major strategies have emerged which allowed for the development of emissive Pt(II) complexes with diimine or triimine ligands. The first strategy relies on raising the energy of the d−d state(s) via introduction of very strong ligand field groups, such as acetylide[34,38−55] or cyanide[56] co-ligands, while retaining the predominantly ligand-to-ligand charge-transfer character of the emissive excited state. Alternatively, high emission quantum yields and long lifetimes can be achieved by changing the nature of the lowest excited state from MLCT/LLCT to intraligand charge-transfer (ILCT) or $\pi-\pi^*$ via modification of the terpyridine ligand in $[Pt(tpy)Cl]^+$.[57−62]

The number of square-planar Pt(II) diimine thiolate/phenolate complexes reported that luminesce in solution is limited mainly to those containing chelating dithiolate ligands such as 1,2-dithiolate[1,13,20,22,23,25,63−67] or 1,1-dithiolates.[68] There are even fewer reports of bis-monothiolate ligands in the literature.[2,32,33,69−71] The poor solubility of most Pt(II) diimine thiolate chromophores (with the exception of some 1,1-dithiolates[68]) in common solvents hinders solution-phase studies and characterization of their electronic properties. We have synthesized Pt(II) chromophores possessing bulky

(11) Ballardini, R.; Balzani, V.; Credi, A.; Gandolfi, M. T.; Venturi, M. *Acc. Chem. Res.* **2001**, 445.
(12) Blaskie, M. W.; McMillin, D. R. *Inorg. Chem.* **1980**, *19*, 3519.
(13) Zuleta, J. A.; Chesta, C. A.; Eisenberg, R. *J. Am. Chem. Soc.* **1989**, *111*, 8916.
(14) Bevilacqua, J. M.; Eisenberg, R. *Inorg. Chem.* **1994**, *33*, 2913.
(15) Connick, W. B.; Geiger, D.; Eisenberg, R. *Inorg. Chem.* **1999**, *38*, 3264.
(16) Cummings, S. D.; Eisenberg, R. *Inorg. Chem.* **1995**, *34*, 2007.
(17) McMillin, D. R.; McNett, K. M. *Chem. Rev.* **1998**, *98*, 1201.
(18) Miller, M. T.; Gantzel, P. K.; Karpishin, T. B. *Inorg. Chem.* **1998**, *37*, 2285.
(19) Miller, M. T.; Gantzel, P. K.; Karpishin, T. B. *J. Am. Chem. Soc.* **1999**, *121*, 4292.
(20) Peck, B. M.; Ross, G. T.; Edwards, S. W.; Meyer, G. J.; Meyer, T. J.; Erickson, B. W. *Int. J. Peptide Protein Res.* **1991**, *38*, 114.
(21) Yersin, H.; Humbs, W. *Inorg. Chem.* **1999**, *38*, 5820.
(22) Shavaleev, N. M.; Accorsi, G.; Virgili, D.; Bell, Z. R.; Lazarides, T.; Calogero, G.; Armaroli, N.; Ward, M. D. *Inorg. Chem.* **2005**, *44*, 61.
(23) Zuleta, J. A.; Bevilacqua, J. M.; Eisenberg, R. *Coord. Chem. Rev.* **1991**, *111*, 237.
(24) Zuleta, J. A.; Bevilacqua, J. M.; Rehm, J. M.; Eisenberg, R. *Inorg. Chem.* **1992**, *31*, 1332.
(25) Zuleta, J. A.; Bevilacqua, J. M.; Proserpio, D. M.; Harvey, P. D.; Eisenberg, R. *Inorg. Chem.* **1992**, *31*, 2396.
(26) Connick, W. B.; Gray, H. B. *J. Am. Chem. Soc.* **1997**, *119*, 11620.
(27) Fleeman, W. L.; Connick, W. B. C. *The Spectrum* **2002**, *15*, 14.
(28) Pettijohn, C. N.; Jochnowitz, E. B.; Chuong, B.; Nagle, J. K.; Vogler, A. *Coord. Chem. Rev.* 1998, 85.
(29) Crites Tears, D. K.; McMillin, D. R. *Coord. Chem. Rev.* **2001**, *211*, 195.
(30) Chassot, L.; von Zelewsky, A.; Sandrini, D.; Maestri, M.; Balzani, V. *J. Am. Chem. Soc.* **1986**, *108*, 6084.
(31) Chang, C. C.; Pfennig, B.; Bocarsly, A. B. *Coord. Chem. Rev.* **2000**, *208*, 33.
(32) Cummings, S. D.; Cheng, L.-T.; Eisenberg, R. *Chem. Mater.* **1997**, *9*, 440.
(33) Base, K.; Tierney, M. T.; Fort, A.; Muller, J.; Grinstaff, M. W. *Inorg. Chem.* **1999**, *38*, 287.
(34) Chan, S. C.; Chan, M. C. W.; Wang, Y.; Che, C. M.; Cheung, K. K.; Zhu, N. Y. *Chem.-Eur. J.* **2001**, *7*, 4180. Furuta, P. T.; Deng, L.; Garon, S.; Thompson, M. E.; Frechet, J.-M. J. *J. Am. Chem. Soc.* **2004**, *126*, 15388.
(35) Geary, E. A. M.; Yellowlees, L. J.; Jack, L. A.; Oswald, I. D. H.; Parsons, S.; Hirata, N.; Durrant, J. R.; Robertson, N. *Inorg. Chem.* **2005**, *44*, 242
(36) Zhang, Y.; Ley, K. D.; Schanze, K. S. *Inorg. Chem.* **1996**, *35*, 7102.
(37) Kumar, L.; Puthraya, K. H.; Srivastava, T. S. *Inorg. Chim. Acta* **1984**, *86*, 173.
(38) Yang, Q. Z., Tong, Q. X., Wu, L. Z., Wu, Z. X., Zhang, L. P., Tung, C. H., *Eur. J. Inorg. Chem.* **2004**, 1948.
(39) Yam, V. W. W.; Tang, R. P. L.; C., W. K. M.; K., C. K. *Organometallics* **2001**, *20*, 4476.
(40) Guo, F. Q.; Sun, W. F.; Liu, Y.; Schanze, K. *Inorg. Chem.* **2005**, *44*, 4055.
(41) Hissler, M.; Connick, W. B.; Geiger, D. K.; McGarrah, J. E.; Lipa, D.; Lachicotte, R. J.; Eisenberg, R. *Inorg. Chem.* **2000**, *39*, 447.
(42) Hissler, M.; McGarrah, J. E.; Connick, W. B.; Geiger, D. K.; Cummings, S. D.; Eisenberg, R. *Coord. Chem. Rev.* **2000**, *208*, 115.
(43) Hua, F.; Kinayyigit, S.; Cable, J. R.; Castellano, F. N. *Inorg. Chem.* **2005**, *44*, 471.
(44) Kang, Y. J.; Lee, J.; Song, D. T.; Wang, S. N. *Dalton Trans.* **2003**, 3493.
(45) McGarrah, J. E.; Eisenberg, R. *Inorg. Chem.* **2003**, *42*, 4355.
(46) Pomestchenko, I. E.; Castellano, F. N. *J. Phys. Chem. A* **2004**, *108*, 3485.
(47) Pomestchenko, I. E.; Luman, C. R.; Hissler, M.; Ziessel, R.; Castellano, F. N. *Inorg. Chem.* **2003**, *42*, 1394.
(48) Wadas, T. J.; Chakraborty, S.; Lachicotte, R. J.; Wang, Q. M.; Eisenberg, R. *Inorg. Chem.* **2005**, *44*, 2628.
(49) Whittle, C. E.; Weinstein, J. A.; George, M. W.; Schanze, K. S. *Inorg. Chem.* **2001**, *40*, 4053.
(50) Yam, V. W. W. *C. R. Chim.* **2005**, *8*, 1194.
(51) Yam, V. W. W.; Tang, R. P. L.; Wong, K. M. C.; Cheung, K. K. *Organometallics* **2001**, *20*, 4476.
(52) Yang, Q. Z.; Wu, L. Z.; Wu, Z. X.; Zhang, L. P.; Tung, C. H. *Inorg. Chem.* **2002**, *41*, 5653.
(53) Siemeling, U.; Bausch, K.; Fink, H.; Bruhn, C.; Baldus, M.; Angerstein, B.; Plessow, R.; Brockhinke, A. *Dalton Trans.* **2005**, 2365.
(54) Shavaleev, N. M.; Moorcraft, L. P.; Pope, S. J. A.; Bell, Z. R.; Faulkner, S.; Ward, M. D. *Chem.-Eur. J.* **2003**, *9*, 5283.
(55) Shavaleev, N. M.; Bell, Z. R.; Easun, T. L.; Rutkaite, R.; Swanson, L.; Ward, M. D. *Dalton Trans.* **2004**, 3678.
(56) Wilson, M. H.; Ledwaba, P. L.; Field, J. S.; McMillin, D. R. *Dalton Trans.* **2005**, *16*, 2754.
(57) Yip, H. K.; Cheng, L. K.; Cheung, K. K.; Che, C.-M. *J. Chem. Soc., Dalton Trans.* **1993**, 2933.
(58) Wilson M. H.; Ledwaba, L. P.; Field, J. S.; McMillin, D. R., *Dalton Trans.* **2005**, 2754
(59) Michalec, J. F.; Bejune, S. A.; Cuttell, D. G.; Summerton, G. C.; Gertenbach, J. A.; Field, J. S.; Haines, R. J.; McMillin, D. R. *Inorg. Chem.* **2001**, *40*, 2193.
(60) Yam, V. W. W.; Wong, K. M. C.; Zhu, N. Y. *Angew. Chem., Int. Ed.* **2003**, *42*, 1400.
(61) Lu, W.; Mi, B. X.; Chan, M. C. W.; Hui, Z.; Che, C.-M.; Y., Z. N.; Lee, S. T. *J. Am. Chem. Soc.* **2004**, *126*, 4958.
(62) Moore, J. J.; Nash, J. J.; Fanwick, P. E.; McMillin, D. R. *Inorg. Chem.* **2002**, *41*, 6387.
(63) Barigelletti, F.; Sandrini, D.; Maestri, M.; Balzani, V.; von Zelewsky, A.; Chassot, L.; Jolliet, P.; Maeder, U. *Inorg. Chem.* **1988**, *27*, 3644.
(64) Camassei, F. D.; Ancarani-Rossiello, F. *J. Luminescence* 1973, *8*, 71.
(65) Vogler, A.; Kunkely, H. *J. Am. Chem. Soc.* **1981**, *103*, 1559.
(66) Vogler, C.; Schwederski, B.; Klein, A.; Kaim, W. *J. Organomet. Chem.* **1992**, *436*, 367.
(67) Webb, D. L.; Rossiello, D. L. *Inorg. Chem.* **1971**, *10*, 2213.
(68) Huertas, S.; Hissler, M.; McGarrah, J. E.; Lachicotte, R. J.; Eisenberg, R. *Inorg. Chem.* **2001**, *40*, 1183.

phenolate or thiolate ligands as a salient feature. This imparts solubility over a wide range of solvent polarities, enabling one to systematically probe the electronic structure. Our strategy is also amenable to determining the affect of donor atom (S vs O), ligand coordination (di- vs bis-mono), and electron donating/withdrawing properties of the ligand on the electronic structure of square-planar d^8 chromophores.

Specifically, we are exploiting two routes to increase the solubility of Pt(II) chromophores while retaining structural homology about the platinum center. First, bulky *tert*-butyl groups are introduced to the periphery of the phenolate/thiolate ligands to prevent molecular stacking from either metal-to-metal or ligand-to-ligand interactions, a reoccurring observation with platinum(II) diimine complexes.[15,19,28,72,73] Bulky functional groups such as *tert*-butyl, isopropyl, or phenyl-*tert*-butyl have been used successfully to prevent self-association or dimerization of metal complexes designed for enhanced catalysis and luminescence.[12,19,74] The second route capitalizes on the large 3-dimensional structure of thiocarboranes. The bulky electron-withdrawing closo-boranes are particularly suited for this use since these structures possess high chemical and thermal stability, and once bound to a metal center, thiocarboranes are expected to act as strong field ligands, thus opening a possibility for enhanced emission properties in solution.

Herein we report a series of structurally similar Pt(II) diimine chromophores **1**−**6** (Scheme 1), characterized by X-ray crystallography and multinuclear (^{1}H, ^{13}C, and ^{195}Pt) NMR, as well as absorption, emission, (spectro)electrochemistry, and EPR spectroscopy. The electronic structure of these chromophores was altered by varying the (i) oxygen and sulfur donor ligands; (ii) electron-donating properties of the thiolate/phenolate ligands; and (iii) bis- and di-coordination modes. The unique reversible nature of the oxidation process of Pt(dpphen)(3,5-di-*tert*-butyl-cathecolate), **5**, has allowed for a direct probing of Pt(II) orbital contribution into the HOMO of this chromophore by EPR spectroscopy. Absorption, emission, UV/vis (spectro)electrochemical studies have revealed the same nature of the lowest excited state in this series of chromophores while allowing for significant tuning of absorption and emission energies and redox properties in the excited state.

Results and Discussion

Synthesis. The general synthetic route to the sterically crowded Pt(II) diimine chromophores containing both oxygen or sulfur donor ligands is shown in Scheme 1. Treatment of the phenolate or thiolate ligand with base in the presence of Pt(dpphen)Cl_2 affords the following complexes: 4,7-diphenyl-1,10-phenanthroline 3,5-di-*tert*-butylbenzene-1,2-dithiolate platinum(II), [Pt(dpphen)(dtbdt)], **1**; 4,7-diphenyl-1,10-phenanthroline bis-4-*tert*-butylbenzenethiolate platinum(II), [Pt(dpphen)$(tbt)_2$], **2**; 4,7-diphenyl-1,10-phenanthroline-[1,2-dithiolato-1,2-dicarba-*closo*-dodecaborane(12)] platinum(II), [Pt(dpphen)(dtoc)], **3**; 4,7-diphenyl-1,10-phenanthroline-bis-[1-thiolato-1,2-dicarba-*closo*-dodecaborane(12)] platinum(II), [Pt(dpphen)$(toc)_2$], **4**; 4,7-diphenyl-1,10-phenanthroline 3,5-di-*tert*-butylbenzene-1,2-catecholate platinum(II), [Pt(dpphen)(dtbc)], **5**; and 4,7-diphenyl-1,10-phenanthroline bis-4-*tert*-butylphenolate platinum(II) [Pt(dpphen)$(tbp)_2$], **6**. The phenolate and catecholate ligands, 4-*tert*-butyl-phenolate (**13**) and 3,5-di-*tert*-butyl-catecholate (**12**) described are commercially available. The thiolate ligands 3,5-di-*tert*-butyl-benzene dithiolate (**8**) and 4-*tert*-butyl-thiophenol (**9**) were synthesized in accordance with their respective literature procedures.[75,76] The synthetic procedure for carboranes **10** and **11** are reported elsewhere.[77]

Scheme 1. Synthesis of Pt(II) 4,7-diphenyl-1,10-phenanthroline-thiolates and Phenolates, **1**−**6**

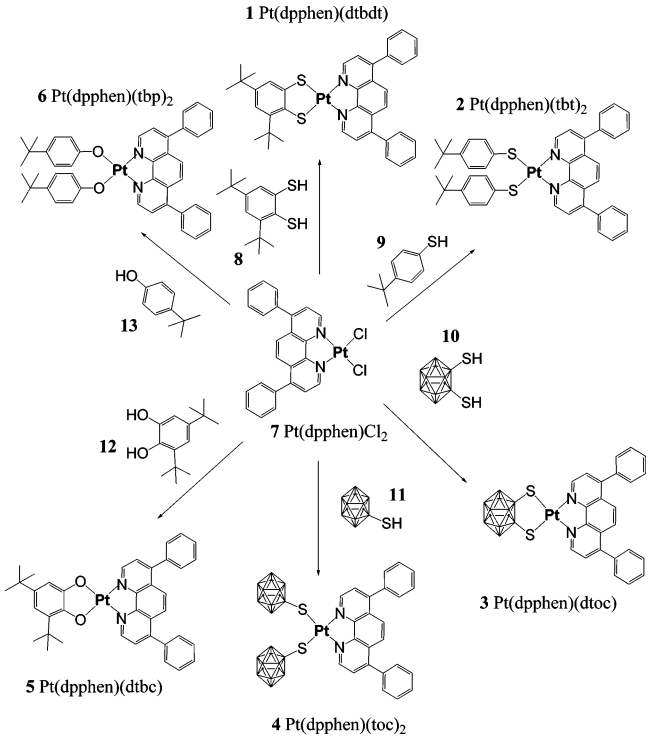

X-ray Crystal Structure of Pt(dpphen)(dtbdt), 1. Slow evaporation of a benzene solution of **1** gave dark blue crystals ($0.40 \times 0.08 \times 0.01$ mm^3) suitable for X-ray analysis. The crystal-structure data for **1**, along with the data for the monodentate analogue, **4**, reported previously[69] and included for comparison, are summarized in Table 1. The ORTEPII thermal ellipsoid plot of **1**, drawn at 50% probability, is shown in Figure 1. The key bond lengths and angles around the central platinum atom in **1** and **4** are displayed in Figure 2. The geometry about the central platinum metal in both **1**

(69) Base, K.; Grinstaff, M. W. *Inorg. Chem.* **1998**, *37*, 1432.
(70) Weinstein, J. A.; Zheligovskaya, N. N.; Lileev, I. V.; Galin, A. M.; Mel′nikov, M. Y. *Russ. J. Inorg. Chem. (Transl. of Zh. Neorg. Khim.)* **1998**, *43*, 1361.
(71) Weinstein, J. A.; Zheligovskaya, N. N.; Mel′nikov, M. Y.; Hartl, F. *J. Chem. Soc., Dalton Trans.* 1998, 2459.
(72) Baley, J. A.; Miskowski, V. M.; Gray, H. B. *Inorg. Chem.* **1993**, *32*, 369.
(73) Kunkely, H.; Vogler, A. *J. Am. Chem. Soc.* **1990**, *112*, 5625.
(74) McMillin, D. R.; Kirchhoff, J. R.; Goodwin, K. V. *Coord. Chem. Rev.* **1985**, *64*, 83.
(75) Sellmann, D.; Prechtel, W.; Knock, F.; Moll, M. *Z. Naturforsch.* **1992**, *47b*, 1411.
(76) Strating, J.; Backer, H. J. *Recl. Trav. Chim. Pays-Bas* **1950**, *69*, 638.
(77) Smith, H. D.; Obenland, C. O.; Papetti, S. *Inorg. Chem.* **1996**, *35*, 1013.

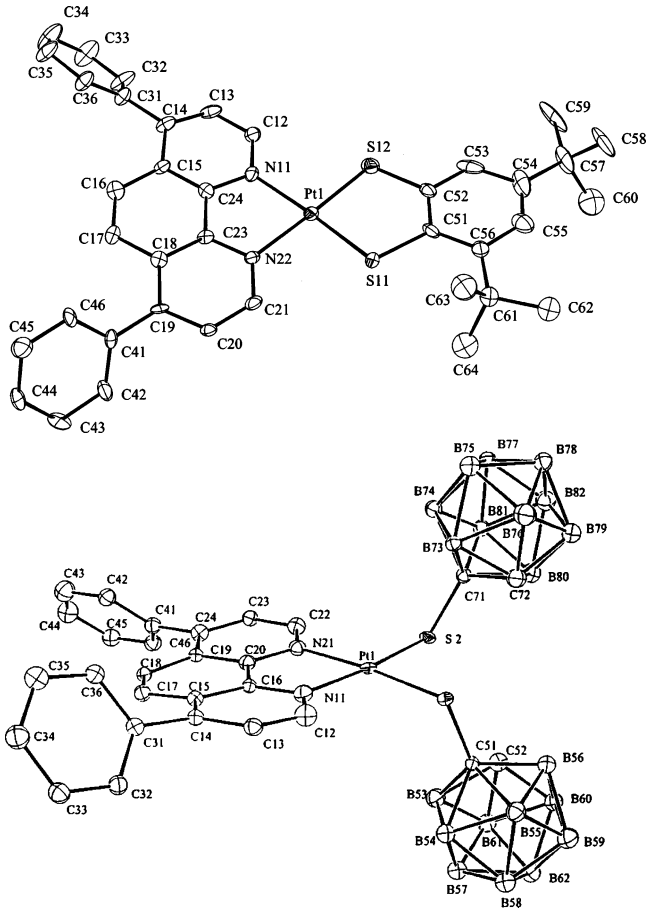

Figure 1. a. An ORTEPII diagram (50% probability ellipsoids) of Pt(dpphen)(dtbdt), **1**, showing the atomic numbering system. H atoms are not shown. **b**. An ORTEPII diagram (50% probability ellipsoids) of Pt(dpphen)(toc)$_2$, **4**. H atoms are not shown.[69]

Table 1. X-ray Crystallographic Data for **1** and **4**

compound	**1**	**4**
formula	$PtC_{48.5}H_{46.5}N_2S_2$	$PtC_{28}H_{40}B_{20}N_2S_2Cl_2$
fw (g mol^{-1})	919.62	960.94
color	dark blue	Yellow
shape	plates	plates
cryst syst	monoclinic	monoclinic
space group	*C*2/*c*	$P2_1/a$
a, (Å)	36.080(14)	16.9705(8)
b, (Å)	14.323(9)	12.9105(6)
c, (Å)	36.672(17)	18.9109(9)
β (deg)	112.063(1)	99.5730(10)
V, (Å^3)	17563(15)	4085.6(3)
ρ_{calcd} (g cm^{-3})	1.387	1.526
Z	16	4
λ, Å	3.31	3.68
temp (K)	173	173
total no. of reflns measured	29 487	21 213
no. of unique reflns	14 492	7240
no. of reflns with $I_{net} > 2.5\rho(I_{net})$	8244	5470
GOF	1.50	1.46
R	0.053	0.058
R_w	0.058	0.077

and **4** is square planar with very little torsional deformation. The structure of **1** reveals an asymmetric curvature of the molecule with regard to the plane formed by the metal center and chelating atoms. As shown in Figure 3, there is an upward bend in the molecule about the two sulfur atoms. This most likely arises from the slightly strained five-membered-ring structure formed. The same observation has been made

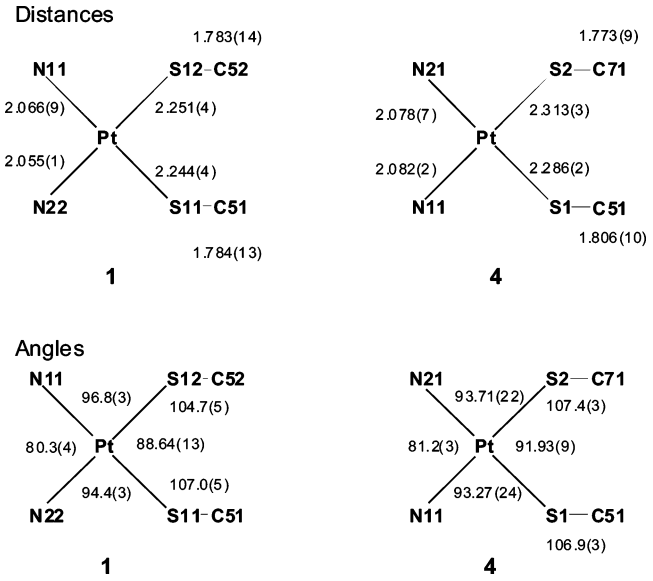

Figure 2. The key bond lengths and angles around the central platinum atom in Pt(dpphen)(dtbdt), **1**, and Pt(dpphen)(toc)$_2$, **4**, complexes.

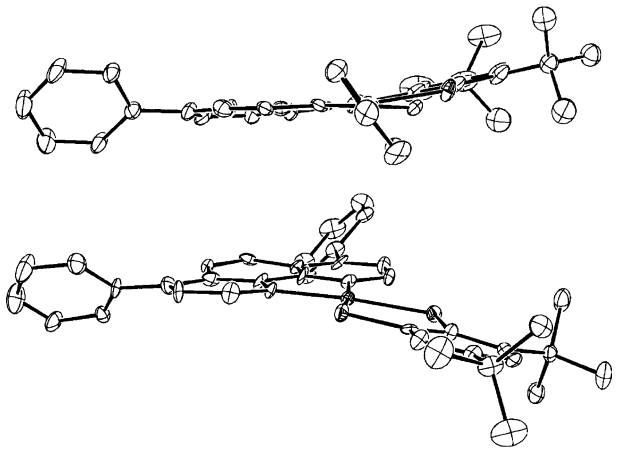

Figure 3. An ORTEPII diagram (50% probability ellipsoids) of Pt(dpphen)(dtbdt), **1**, showing the upward bend in the molecule about the two sulfur atoms. H atoms are not shown.

previously for other Pt(II) dithiolates which feature five-membered [C−S−Pt−S−C] rings. For example, the dihedral angle between the [NN−Pt−SS] plane and the [S−C−C−S] plane of the thiolate ligand is 3° for (4,4′-dimethyl-2,2′-bpy)(1,2-dimethoxycarbonylethylene-1,1-dithiolato)Pt, [14] 4.5° for Pt(bpy)(benzene-1,2-dithiol),[26] and 7° for (bpy)(6,7-dihydro-5H-1,4-dithiepin-2,3-dithiolato)Pt.[78]

As summarized in Figure 2, the Pt−S and Pt−N diimine bond lengths in Pt(dpphen)(dtbdt) are 2.251(4), 2.244(4), 2.066(9), and 2.055(10) Å, respectively, and in the range of bond lengths typical for other Pt diimine dithiolate structures.[14,78] In the Pt(II) bis-monothiolate complex **4**, the Pt−S carborane and Pt−N diimine bond lengths are slightly longer: 2.313(3), 2.286(2), 2.082(8), and 2.078(7) Å, respectively. The Pt−S distances of Pt(dpphen)(toc)$_2$ are in agreement with previously reported bis-monothiolate struc-

(78) Zuo, J. L.; Xiong, R. G.; You, X. Z.; Huang, X. Y. *Inorg. Chim. Acta* **1995**, *237*, 177.

Table 2. ^{1}H NMR Assignments of Pt(dpphen)D Complexes[a]

complex D = position	**1** (dtbdt) δ, (mult, J/Hz)	**2** $(tbt)_2$ δ, (mult, J/Hz)	**3** (dtoc)[b] δ, (mult, J/Hz)	**4** $(toc)_2$[b,c] δ, (mult, J/Hz)	**5** (dtbc) δ, (mult, J/Hz)	**6** $(tbp)_2$ δ, (mult, J/Hz)
9	9.41 (d, 5.5)	10.13 (d,5.5)	8.97	10.21(d,5.5)	9.46 (d, 5.5)	9.33
2	9.31 (d, 5.5)		(d, 5.5)		9.41 (d, 5.5)	(d, 5.5)
8	7.62 (d)	7.82	7.78	8.08 (d, 5.5)	7.68 (d, 5.5)	7.80
3	7.65 (d)	(d, 5.5)	(d, 5.5)		7.66 (d, 5.5)	(d, 5.5)
5, 6	7.99 (m)	8.06 (s)	8.07 (s)	8.13 (s)	7.96 (s)	8.05 (s)
	7.96 (m)					
2′,6′ 2″,6″	7.46 (m)	7.61 (m)	~7.59 [m]	~7.65 (m)	~7.58 (m)	~7.61 (m)
	7.53 (m)					
3′,5′ 3″,5″	7.51 (m)	7.61 (m)	~7.61 [m]	~7.65 (m)	~7.58 (m)	~7.61 (m)
	7.57 (m)					
4′, 4″	7.55 (m)	7.61 (m)	~7.60 [m]	~7.65 (m)	~7.59 (m)	~7.61 (m)
D2, D6[d]		7.57				7.22
		(d, 8.4)				(d, 8.8)
D3[e]	6.93 (m)	7.00			6.48 (m)	7.07
		(d, 8.4)				(d, 8.8)
D5	7.23 (m)				6.68 (m)	
4^{t}Bu Me	1.35 (s)	1.23 (s)			1.33 (s)	1.25 (s)
2^{t}Bu Me	1.67 (s)				1.55 (s)	

[a] 1H NMR chemical shift relative to internal TMS taken from 600 MHz NMR data at 25 °C. [b] $B_{10}H_{10}$ protons appear as broad signal near 2.53 ppm in **3** and 2.50 ppm in **4**. [c] Carborane CH appears at 4.65 ppm. [d] In symmetrical complexes **2** and **6**, the D-2′/D-6′ signals are isochronous with D-2 and D-6. [e] In symmetrical complexes **2** and **6**, the D-5, D-3′, and D-5′ signals are isochronous with D-3.

tures, $Pt(dbbpy)(S\text{-}4\text{-}py)_2$,[79] and $Pt(bpy)(4\text{-}CN{-}C_6F_4{-}S)_2$ (2.282(3)/2.296(3) Å)[2] but are longer than those reported for the dithiolate[14,80] systems, indicating less covalent character of the Pt−S bond in the former case. However, the slight lengthening of the $C_{carborane}$−thiol bond from 1.729(4) Å in carborane−thiolate[81] to 1.806(10) Å in $Pt(dpphen)(toc)_2$ indicates good conjugation in the Pt−S−$C_{carborane}$ system. Structural studies on *o*-carborane and its derivatives show that skeletal C−C bonds in the closo icosahedron are in the range of 1.63−1.74 Å for the neutral trisulfide 1,1′-S_3-(2-C_6H_5-1,2-$C_2B_{10}H_{10}$). The skeletal C−C bonds in Pt(dpphen)-$(toc)_2$ are in the range of a closo icosahedron (i.e., 1.606(13) and 1.637(14)Å for C(51)−C(52) and C(71)−C(72), respectively), whereas the parent [1-*S*-2-C_6H_5-1,2-$C_2B_{10}H_{11}]^-$ anion has a skeletal C−C distance of 1.835 Å.

Both Pt chromophores are not closely packed in the unit cell, and this is a likely consequence of the bulky *tert*-butyl groups or carborane cage. There are 16 molecules in the large unit cell of **1** (see the Supporting Information for detail), while there are only four in the unit cell of **4**.[69] The lack of molecular stacking observed in the crystal structure is noteworthy since Pt(II) complexes are well-known to stack in the solid state, with short Pt−Pt or π-to-π (3.24 and 3.51 Å, respectively) distances.[80,82,83] The Pt−Pt distances for **1** and **4** are 4.25 and 8.48 Å, respectively, clearly indicating that the bulky substituents on the ligands are preventing stacking of the chromophores in the crystal.

NMR Spectroscopy. To gain insight into the structures of all six Pt(II) chromophores, **1**−**6**, in solution, ^{1}H, ^{13}C, and ^{195}Pt NMR studies[84−90] have been performed (see the Supporting Information for complete assignment of the resonances). These six Pt(II) complexes possess a common substituted phenanthroline acceptor group (dpphen) and differ

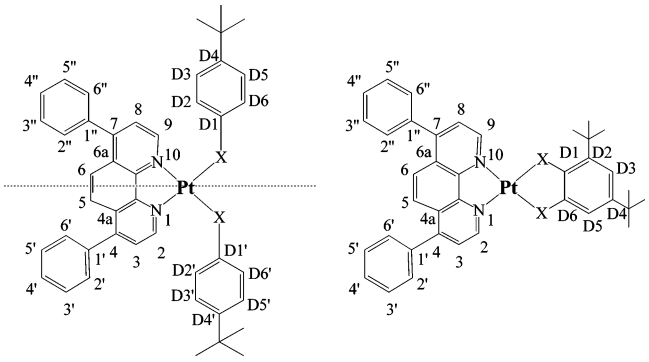

Figure 4. Schematic representation of (left panel) Pt(II) complexes **2** and **6** with the symmetry axis indicated and (right panel) complexes **1** and **5** with asymmetric ^{t}Bu groups on the donor ring. The atom numbering scheme for the NMR assignment are as indicated. "D" represents atoms from the donor thiolate or catecholate rings.

by the nature of the donor ligand (designated D). Complexes **2**−**4** and **6** are symmetric about an axis which bisects the phenanthroline ring, the platinum atom, and the thiolate (or phenolate) ligand(s). The proton assignments are summarized in Table 2, and a complete description of the analysis is found in the Supporting Information. Of particular note is the proton spectra obtained from chromophores **1** and **5**. The lack of symmetry for **1** and **5** results in distinct environments for H-2, H-9, H-3, H-8, H-5, and H-6 (Table 2) and their corresponding carbon atoms (Figure 5 and Supporting Information).

Lack of symmetry in chromophores **1** and **5** also leads to separate ^{13}C NMR signals from the "top" and "bottom" portions of the phenanthroline ring (Figure 5). Steady-state 1-dimensional (1D) NOE experiments on chromophore **5** at

(79) Paw, W.; Lachicotte, R. J.; Eisenberg, R. *Inorg. Chem.* **1998**, *37*, 4139.
(80) Connick, W. B.; Marsh, R. E.; Schaefer, W. P.; Gray, H., B. *Inorg. Chem.* **1997**, *36*, 913.
(81) Coult, R.; Fox, M. A.; Gill, W. R.; Wade, K. *Polyhedron* **1992**, *11*, 2717.
(82) Connick, W. B.; Henling, L. M.; Marsh, R. E.; Gray, H. B. *Inorg. Chem.* **1996**, *35*, 6261.
(83) Osborn, R. S.; Rogers, D. *J. Chem. Soc., Dalton. Trans.* **1974**, 1002.
(84) Bax, A.; Freeman, R.; Morris, G. A. *J. Magn. Reson.* **1981**, *42*, 164.
(85) Bax, A.; Subramanian, S. *J. Magn. Reson.* **1986**, *67*, 656.
(86) Bax, A.; Summers, M. F. *J. Am. Chem. Soc.* **1986**, *108*, 2093.
(87) Garbow, J. R.; Wietekamp, D. P.; Pines, A. *Chem. Phys. Lett.* **1982**, *93*, 504.
(88) Pregosin, P. S. *Coord. Chem. Rev.* **1982**, *44*, 247.
(89) Shaka, A. J.; Barker, P. S.; Freeman, R. *J. Magn. Reson.* **1985**, *64*, 547.
(90) Summers, M. F.; Marzilli, L. G.; Bax, A. *J. Am. Chem. Soc.* **1986**, *108*, 4285.

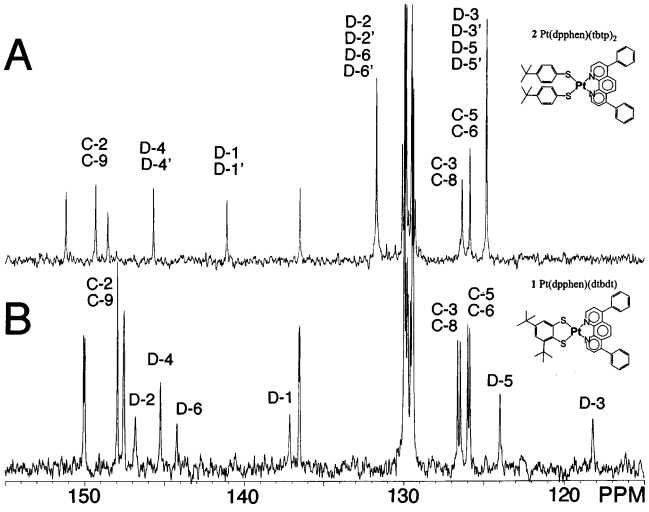

Figure 5. Partial 150 MHz ^{13}C NMR spectra at 25 °C showing aromatic ^{13}C NMR resonances of thiolate Pt complexes **2** (top panel) and **1** (bottom panel). Due to the axis of symmetry in complex **2**, the 36 aromatic carbons are simplified to 14 carbon resonances. Lack of symmetry in complex **1** leads to separate phenanthroline C-2/C-9, C-3/C-8, and C-5/C-6 carbon signals. The six carbons of the donor dithiolate ring yield six broad and low-amplitude ^{13}C signals (range of line widths 4−15 Hz for D-1 to D-6). The D-1 and D-6 signals in complex **5** have similar line widths to the D-1 and D-6 signals of **1** (7−8 Hz), but the D-2 to D-5 resonances are considerably broader (30−40 Hz).

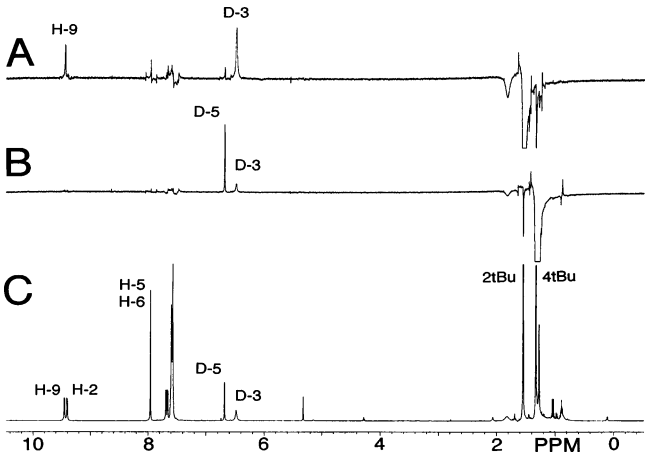

Figure 6. 500 MHz NMR spectra of Pt(II) complex **5** at 25 °C. (A−B) difference NOE spectra: (A) irradiation of the 2-^{t}Bu methyl gives selective NOE enhancements at the D-3 proton of the donor phenolate ring and one proton of the acceptor phenanthroline ring which corresponds to H-9 in the numbering scheme used. (B) Excitation of the 4-^{t}Bu methyl reveals enhancements at D-5 and D-3 of the donor phenolate ring. (C) ^{1}H NMR spectrum.

25 °C (Figure 6) show lack of a mutual NOE between the 2-^{t}Bu and 4-^{t}Bu methyl groups, implying that those are oriented away from each other and possibly located on opposite faces of the donor ring resulting from steric hindrance. Taking into account the generally larger ^{13}C line widths of D-2 to D-5 compared to D-1 and D-6 (attached to S− or O−), the specific line broadening of D-3, and the observation of a specific NOE indicating proximity of the donor 2-^{t}Bu group to the acceptor H-9 phenanthroline proton, the overall NMR data suggest a working model with distorted or bent donor ring where a 2-^{t}Bu group on the "top" face approaches H-9 of the phenanthroline ring to yield a distinct

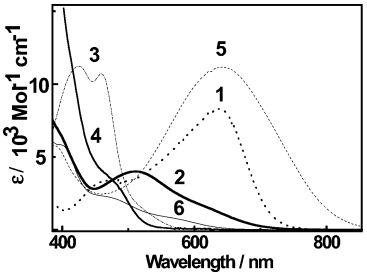

Figure 7. Electronic absorption spectra of **1**−**6** in $CHCl_3$ at room temperature.

NOE and the D-3 proton is broadened from steric collisions with both tBu methyl groups.

The ^{195}Pt NMR data are shown in Table 4. The shift in the ^{195}Pt resonance to less negative values from compound **1** to compound **6** reflects an increase in the electron-withdrawing ability of the thiolate/phenolate ligand along this row. As will be discussed below, the trend in the ^{195}Pt resonances also correlates with the trend in oxidation peak potentials of **1**−**6**. Of particular note is the 300 ppm upfield shift in the ^{195}Pt NMR signal of complex **3** compared to that of complex **4.** This shift gives evidence for the ^{195}Pt atom to be more electronically shielded in **4** likely due to a better overlap of platinum d orbitals with sulfur p orbitals. However, the H-2, H-9 and H-3, H-8 NMR signals of the phenanthroline ring of complex **4** are shifted to lower field compared to those of complex **3**, showing that there is aconcomitant decrease in the electronic shielding in the phenanthroline ring with the increase in electronic shielding at the Pt atom. We believe that the differences in shielding of phenanthroline hydrogens can be explained by the enhanced electron-withdrawing effect of two *o*-carborane cages in **4**.

Visible Absorption Spectroscopy. Solutions of complexes **1**−**6** exhibit an intense absorption at 290 nm due to the π-to-π^* transition of diphenylphenanthroline and a second absorption at longer wavelength with extinction coefficient values of the order of 10^3 dm^3 mol^{-1} cm^{-1} (Table 3, Figure 7). The energy and the extinction coefficient of this visible absorption band depends on the electron withdrawing/donating ability of the ligand, the coordination geometry (di vs bis ligation), and the nature of donor atom, as shown in Table 3. The energy of the transition increases on going from electron donating *tert*-butyl derivatives to the strongly electron-withdrawing carboranes (e.g, **1** to **3** or **2** to **4**). In all cases, the absorption shifts to lower energy from bis- to di-coordination. Compound **4** possesses the highest-energy visible absorption band, which is partly obscured by π-to-π^* transition of the diphenyl-phenanthroline, and **5** possesses the lowest-energy absorption. These observations demonstrate thiolate/phenolate ligand orbital participation in the occupied molecular orbital responsible for this electronic transition. Within the same structural motif (**5** vs **1**), changing from oxygen to sulfur slightly (550 cm^{-1}) shifts the absorption to higher energy.

The extinction coefficients for the lowest absorption band are much higher for the complexes with bidentate thiolate ligands than for those with the monodentate ligands (8000−

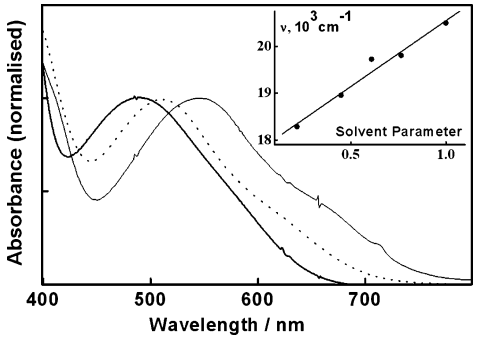

Figure 8. Electronic absorption spectra of **2** in acetonitrile (thick solid line), $CHCl_3$ (dashed line), and benzene (thin solid line). The plot of absorption energy (in cm^{-1}) vs solvent parameter[1] is shown in the insert.

11000 vs 2250−4000 L mol^{-1} cm^{-1}). This is likely due to better mixing with the metal d orbitals for the former. Interestingly, solutions of **3** and **4** in DMF, $CHCl_3$, CH_2Cl_2, and C_6H_6 are stable to irradiation into the long-wavelength absorption band which can be contrasted with the previously reported reactivity of Pt(diimine)(dithiolate) complexes such as Pt(bpy)(tdt).[65,91] The lowest-energy absorption bands in **1**−**6** show negative solvatochromic behavior, that is, the band position shifts to lower energies with an increase of solvent polarity. Such behavior is indicative of a significant difference between the ground- and excited-state dipole moments and is typical for MLCT/LLCT transitions.[92,93] A representative example of the solvatochromic behavior of these chromophores is shown in Figure 8 for **2**.

A linear correlation has been observed between the energy of this lowest absorption band and the solvent polarity parameter value based on the energy of the [charge-transfer-to-diimine] transition in Pt(dbbpy)(tdt) (dbbpy = 4,4′-di-*tert*-butyl-2,2′-bipyridine, tdt = toluene-3,4-dithiolate).[1] The slope of the linear correlation (Figure 8) gives a so-called solvatochromic shift (Table 3); the values obtained for **1**−**6** are within the range observed for charge-transfer transitions. The pronounced solvatochromism, as well as thiolate/phenolate ligand effect on the energy of the lowest absorption band, indicates the charge-transfer character of the corresponding electronic transition.

Most of the compounds studied also exhibit a shoulder at 3000−3900 cm^{-1} lower in energy than the main transition (Table 3), which is characterized by an oscillator strength several times smaller than that of the main charge-transfer band discussed above. It has been shown for other Pt(II) compounds that this singlet−triplet transition can be of considerable intensity due to the presence of the heavy atom effect induced by the Pt(II) center.[36] We hence tentatively assign the low-energy absorbance to a singlet−triple satellite to singlet−singlet charge-transfer transition described above.

(Spectro)electrochemistry. The redox behavior of the Pt^{II} 4,7-diphenyl-1,10-phenanthroline complexes with thiolate and phenolate ligands, **1**−**6**, was studied in DMF by cyclic voltammetry and UV/vis (spectro)electrochemistry to elucidate the nature of the frontier orbitals in these chromophores. The redox potentials of compounds **1**−**6** are summarized in Table 4. Representative cyclic voltammograms are shown in Figure 9 for **2**, **5**, and **3**. The absorption maxima of the electrochemically generated radical anions of compounds **1**−**6** and Pt(dpphen)Cl_2 and that of the radical cation of **5** registered in DMF at 273 K are summarized in Table 5.

Reduction. All the complexes investigated exhibit a reversible one-electron first reduction process in the region between −1.49 and −1.68 V. The complexes with bidentate thiolate or phenolate ligands display the half-wave potential of the first reduction at ca. 60 mV more negative than their monodentate analogues (**5** vs **6** and **1** vs **2**). There is only a small (0.02 V) negative shift in the first reduction potential when an S-containing ligand is replaced by an O-containing analogue (**1** vs **5**, **2** vs **6**). Thus, neither the mode of coordination (bis vs di), nor the type of donor atom (S vs O), nor the electron withdrawing/donating properties of the ligand substantially effect the magnitude of the first reduction potential of the complexes, which is close to that of the first reduction potential of Pt(dpphen)Cl_2 (−1.55 V). We therefore conclude that the first reduction is predominantly localized on the diimine ligand and that the LUMO is of mainly diimine character. The small gradual positive shift in the reduction potential from **1** to the complex containing two thiocarboranes (**4**) is due to a decrease in the electron-donating capability of the thiolate/phenolate ligand, which increases diimine-to-platinum σ-donation.

The second reduction process, detected in the region from −2.05 to −2.28 V, is virtually insensitive to the nature of the donor ligand and very similar to the second reduction process for Pt(dpphen)Cl_2 (−2.17 V). Hence, it is proposed that the second cathodic step is also localized on the diimine ligand.

To obtain better insight in the nature of the LUMO, (spectro)electrochemical experiments were performed for **1**−**6** and Pt(dpphen)Cl_2. For all the compounds investigated, the first reduction process is accompanied by a gradual change in the absorption spectrum, with the formation of new bands across the visible region (Table 5). As a typical example, the spectral changes accompanying the first reduction process of **4** are shown in Figure 10. The position and extinction coefficients of these bands remain virtually unaffected by the nature of the thiolate/phenolate ligand: the spectral profiles of all the $[Pt(dpphen)(RS/RO)]^{-\bullet}$ are remarkably similar to each other (Table 5, Figure 10, insert), and are comparable to that of $[Pt(dpphen)Cl_2]^{-\bullet}$. This establishes that the first reduction process is directed to the π_1*(dpphen), thus supporting the assignment of LUMO as predominately diimine-based for **1**−**6**.

Oxidation. So far, direct spectroscopic probing of the orbital parentage of the HOMO in Pt(II) diimine thiolate/phenolates has not been possible due to the chemical irreversibility of the oxidation process. In line with this fact, all the chromophores studied except the catecholate **5** display an irreversible oxidation wave in DMF solution at 298 K.

(91) Williams, R.; Billig, E.; Waters, J. H.; Gray, H. B. *J. Am. Chem. Soc.* **1966**, *88*, 43.
(92) Lever, A. B. P. *Inorganic electronic spectroscopy*, 2nd ed.; Elsevier: Amsterdam; Oxford, 1984.
(93) Manuta, D. M.; Lees, A. J. *Inorg. Chem.* **1986**, *25*, 3212.

Table 3. Absorption and Emission Data for the Platinum Chromophores **1**−**6**

platinum chromophore ($CHCl_3$ at 25 °C)	λ_{max}^{abs} (nm)	ϵ (mol^{-1} L cm^{-1})	solvatochromic shift, (eV^{-1}) [a]	λ_{max}^{em} (nm)[c]	φ[b]
1 Pt(dpphen)(dtbdt)	634	8300	0.42	710	2.2×10^{-3}
	ca.800 sh	1400			
2 Pt(dpphen)$(tbdt)_2$	510	4000	0.35	660	1.1×10^{-3}
	ca.625 sh	1450			
3 Pt(dpphen)(dtoc)	450	8080	0.34	550	0.13
	ca.520 sh	1400		[640]	[7×10^{-6}]
4 Pt(dpphen)$(toc)_2$	414	3460	0.09	530	0.05
	475	940	0.25	[635]	[1.6×10^{-4}]
5 Pt(dpphen)(dtbc)	657	11 000	0.46	[d]	
6 Pt(dpphen)$(tbp)_2$	470	2250	0.26	556	3.2×10^{-2}
	ca. 575	750			

[a] A gradient of the plot of ν_{max}^{abs} (eV) vs solvent parameter[1] in 2-MeTHF, 77 K. [b] ±20%, measured relative to $[Ru(bpy)_3]Cl_2$ ($\varphi = 0.376$ at 77 K in MeOH glass[94]). [c] Values in square brackets correspond to studies at 298 K in aerated CH_2Cl_2, φ measured relative to $[Ru(bpy)_3]Cl_2$ ($\varphi = 0.028$ in aerated H_2O). [d] No emission was observed between 500 and 800 nm.

Table 4. Electrochemical Data for the Platinum Chromophores **1**−**6**

metal chromophore	$E_{1/2}^{0/-}$	$E_{1/2}^{-/2-}$	E_p^a(ox)	ΔE (Fc/Fc^+) mV	δ ^{195}Pt	ΔE_{redox}, V	E_{emis}, 77 K, cm^{-1} (eV)
5 Pt(dpphen)(dtbc)	−1.66 (70)	−2.28 (70)	−0.07 (70) and 0.56	70	−1992.7	1.63	[b]
1 Pt(dpphen)(dtbdt)	−1.68 (70)	−2.28 (70)	0.05	70	−3517	1.73	13790 (1.71)
2 Pt(dpphen)$(tbt)_2$	−1.62 (70)	−2.22 (70)	0.19	70	−3444.2	1.81	15150 (1.88)
6 Pt(dpphen)$(tbp)_2$	−1.60 (70)	−2.22 (70)	0.40 and 0.73	70	−1816.7	2.00	17990 (2.23)
3 Pt(dpphen)(dtoc)	−1.54 (70)	−2.14 (70)	0.95	70	−3437.9	2.49	18180 (2.25)
Pt(phen)$(C_6F_5{-}S)_2$[c]	−1.61		0.99		−3215		
4 Pt(dpphen)$(toc)_2$	−1.49 (70)	−2.06 (80)	1.05	70	−3142.1	2.54	20040 (2.48)
4[d] Pt(dpphen)$(toc)_2$	−1.57 (70)	−2.05 (90), qr	1.09	70		2.65	20040 (2.48)
Pt(dpphen)Cl_2	−1.55 (70)	−2.17 (70)	0.89	70			

[a] The first and second half-wave reduction potentials, $E_{1/2}^{0/-}$ and $E_{1/2}^{-/2-}$, oxidation potential $E_{1/2}^{0/+}$ or oxidation wave, E_p^a, in V, vs Fc/Fc^+, with anodic/cathodic peak separation given in parentheses. $\Delta E_{redox} = E_p^a - E_{1/2}^{0/-}$, E_{emis} = emission maximum at 77 K is given to be compared with ΔE_{redox}. [b] Emission not detected. [b] From ref 2. [c] In dichloromethane.

Table 5. Electronic Absorption Spectra of the Radical Anions of Pt^{II} 4,7-Diphenyl-1,10-phenanthroline Chromophores **1**−**6** (at 273 K) and of the Radical Cation of [Pt(dpphen)(dtbc)], **5**, (at 243 K) Electrochemically Generated at an OTE, in DMF Solution

metal chromophore	λ_{max}/nm
1 $[Pt(dpphen)(dtbdt)]^{-\bullet}$	272, 283sh, 317sh, 384, 453, 501, 605, 677, 734, 817
2 $[Pt(dpphen)(tbt)_2]^{-\bullet}$	289, 338sh, 426, 497, 610, 660, 716sh, 794
3 $[Pt(dpphen)(dtoc)]^{-\bullet}$	281, 308sh, 334, 369sh, 402, 472sh, 595, 643, 716, 799
4 $[Pt(dpphen)(toc)_2]^{-\bullet}$	268, 295, 317, 336sh, 426, 458sh, 513, 578, 624, 692, 770, 861
5 $[Pt(dpphen)(dtbc)]^{-\bullet}$	284, 307, 365sh, 444sh, 502, 616, 664, 733, 814
6 $[Pt(dpphen)(tbp)_2]^{-\bullet}$	290, 322 sh, 425, 502 sh, 604 sh, 656, 812, 792
$[Pt(dpphen)Cl_2]^{-\bullet}$	325, 357, 441, 475, 591(sh), 635, 709(sh), 790
5 $[Pt(dpphen)(dtbc)]^{+\bullet}$	324sh, 372sh, 478, 608, 660sh

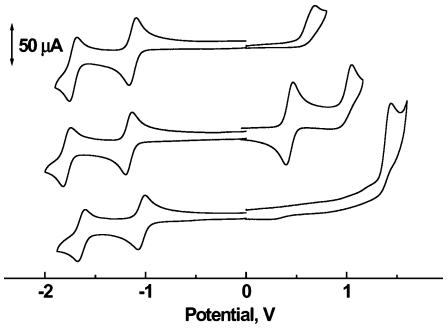

Figure 9. Cyclic voltamograms of 10^{-3} M solution of (a) [Pt(dpphen)$(tbt)_2$], (**2**); (b) [Pt(dpphen)(dtbtc)], (**5**); (c) [Pt(dpphen)(dtoc)], (**3**). DMF, 0.2 M [^{n}Bu$_4$N][BF_4] at 293 K, glassy carbon disk electrode, 100 mV scan rate; *x* axis shows potential vs Fc^+/Fc couple.

Remarkably, the first oxidation of the catecholate chromophore **5** is a reversible one-electron process. *o*-Semiquinone radical anions are known to form stable radical complexes with transition metals and undergo redox reaction

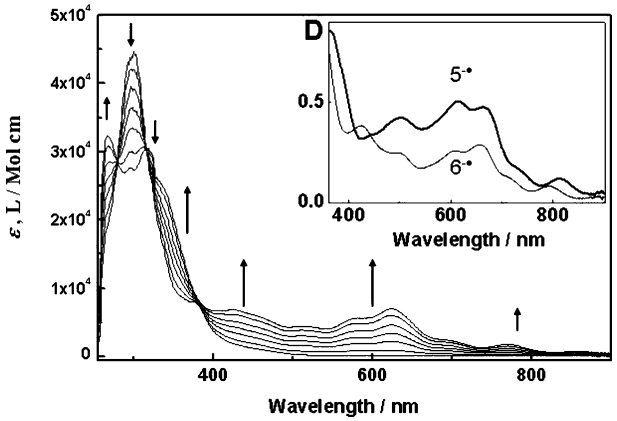

Figure 10. Spectral changes accompanying one-electron reduction process of [Pt(dpphen)$(toc)_2$], **4**, in DMF at 0°C, in the presence of 0.2 M [^{n}Bu$_4$N][BF_4]. Insert: Spectra of radical anions Pt(dpphen)$(dtbc)_2$, $\mathbf{5}^{-\bullet}$ (thick line), and Pt(dpphen)$(tbp)_2$, $\mathbf{6}^{-\bullet}$ (thin line), generated electrochemically in an OTE cell under the same conditions.

while remaining bound to the metal center.[95−98] Reversible thiolate/phenolate-based oxidation has been reported for Pd(2,2′-bipyridine)L (L = 3,5-di-*tert*-butylbenzene-1,2-dithiolate or 1,2-dicathecolate).[99] To the best of our knowledge, **5** represents the first example of such behavior in a Pt(II) diimine thiolate/phenolate complex. Thus, we initiated studies to determine the orbital parentage of the HOMO for this class of complexes.

(94) Demas, J. N.; Crosby, G. A. *J. Am. Chem. Soc.* **1971**, *93*, 2481.
(95) Hartl, F.; Vlcek, A. *Inorg. Chem.* **1996**, *35*, 1257.
(96) Piepont, C. G.; Buchanan, R. M. *Coord. Chem. Rev.* **1981**, *38*, 45.
(97) Piepont, C. G.; Lange, C. W. *Prog. Inorg. Chem.* **1994**, *41*, 331.
(98) Rall, J.; Kaim, W. *J. Chem. Soc., Faraday Trans.* **1994**, *90*, 2905.
(99) Ghosh, P.; Begum, A.; Herebian, D.; Bothe, E.; Hildenbrand, K.; Weyhermuller, T.; Weighardt, K. *Angew. Chem., Int. Ed.* **2003**, *42*, 563.

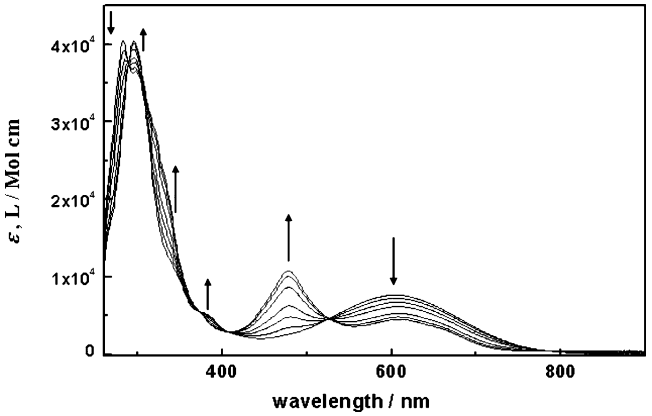

Figure 11. Spectral changes accompanying one-electron oxidation process of [Pt(dpphen)(dtbc)], **5**, in DMF at 243 K, in the presence of 0.2 M [^{n}-Bu_4N][BF_4].

The oxidation peak potential E_p^a (Table 4) is remarkably sensitive to the nature and binding mode of the S− or O− donor ligand. The E_p^a value shifts considerably to negative potentials with increasing donor capacity of the thiolate/phenolate ligand, providing a 1.1 V difference within the series of the chromophores studied. For instance, compounds **3** and **4** possessing thiocarborane derivatives exhibit the most positive oxidation potentials. A change from sulfur to oxygen donor atom alters the electrochemical behavior significantly, shifting the oxidation potentials by ca. 200 mV toward more positive values. The change from mono- to bidentate binding mode leads to a decrease of the oxidation potential. These observations suggest that the HOMO has significant contribution from the orbitals centered at the donor ligand.

The reversible nature of this first oxidation processes observed for the catecholate chromophore **5** allowed for a (spectro)electrochemical investigation of the nature of the HOMO. The formation of a mono-oxidized species (Figure 11) is accompanied by the depletion of the absorption band at 601 nm and the formation of an intense new absorption band at ca. 478 nm. The position of this band is very close to that reported for the semiquinone 3,5-di-*tert*-butylcathecol radical coordinated to the Ni(II) center (472 nm in acetonitrile).[100] This electronic transition has been assigned previously to a d(π)−π* MLCT transition,[95] where the π* orbital of the catecholate semiquinone ligand has $3b_1$ symmetry assuming a C_{2v} point group. These results suggest that the oxidation is centered on the catecholate ligand, thus further supporting the assignment of the HOMO as predominantly phenolate/thiolate ligand based.

EPR Spectroscopy. The nature of the electrochemically generated radical anion and radical cation of **5** was further studied by EPR spectroscopy (Figure 12) to evaluate the extent of Pt orbitals contribution into the frontier orbitals. The EPR spectra of electrochemically generated $\mathbf{5}^{-\bullet}$ and $\mathbf{5}^{+\bullet}$ were recorded in frozen solution at 77 K. There is a clear difference between the EPR spectrum obtained for the radical anion and radical cation of **5** (Figure 12), although both spectra reveal an interaction of the unpaired electron with

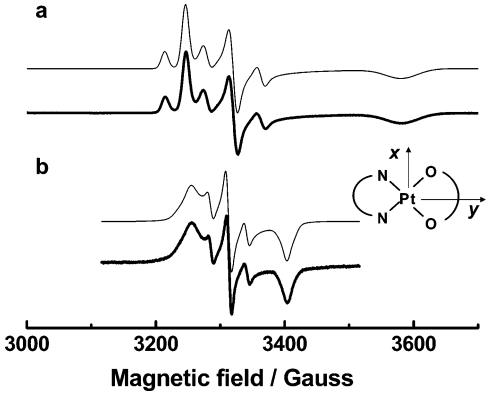

Figure 12. EPR spectra of radical anions of Pt(dpphen)(dtbc)$_2$, **5**, electrochemically generated in DMF at 273 K, recorded at 77 K. The system of coordinates used is shown as an insert. Experimental (thick line) and simulated spectra (thin line) are offset for clarity. **a**. Radical anion, $5^{-\bullet}$, modulation amplitude 10 Gs. Parameters used in simulation (A = hyperfine splitting constant, 10^{-4} cm^{-1}; line width in parentheses, 10^{-4} cm^{-1}): A_{xx}, −86 (11), A_{yy}, −64 (11); A_{zz}, −18 (48); g_{yy} = 2.039, g_{xx} 1.993, g_{zz} 1.848. **b**. Radical cation $5^{+\bullet}$, modulation amplitude 1 Gs. Parameters used in simulation: A_{xx}, 56 (7), A_{yy}, 35 (17), A_{zz}, 22 (11); g_{xx}, 2.002, g_{yy}, 2.038, g_{zz}, 1.948.

Pt nucleus (nuclear spin $I = 0$ (66.2%) and $I = 1/2$ (33.8%), [101] as manifested by the spectral shape and the values of $g_{xx,yy,zz}$ obtained.

The EPR spectrum of radical anion $\mathbf{5}^{-\bullet}$ at 77 K is a superposition of two rhombic EPR spectra, corresponding to the anionic species containing a Pt nucleus with $I = 0$ and 1/2. The overall shape of the EPR spectrum of $\mathbf{5}^{-\bullet}$ is similar to those observed previously[102,103] for several [Pt(diimine)Cl_2]$^{-\bullet}$ complexes. The results of the simulation of the EPR spectra are presented in Figure 12, with the parameters used summarized in the figure caption.

It has been noted previously that in the complexes of the type Pt(diimine)Cl_2 the main contribution of the Pt center to the SOMO of the radical anion comes from $5d_{yz}$ and $6p_z$ orbitals.[102,103] McInnes and Yellowlees[102,103] described an approach which allowed contributions from 5d and 6p Pt orbitals in the SOMO of radical anions [Pt(diimine)Cl_2]$^{-\bullet}$ to be calculated from metal hyperfine splitting constants extracted from the EPR spectra of these species.

To extract contributions of $5d_{yz}$ (a^2) and $6p_z$ (b^2) orbitals in the SOMO of $\mathbf{5}^{-\bullet}$, the following equations were used.[102,103] $A_{xx} = A_s - (4/7)P_d a^2 - (2/5)P_p b^2$; $A_{yy} = A_s + (2/7)P_d a^2 - (2/5)P_p b^2$; $A_{zz} = A_s + (2/7)P_d a^2 + (4/5)P_p b^2$. A_s is the isotropic Fermi constant term. Assuming $5d^8$ configuration of the central atom, the electron nuclear dipolar coupling parameters for 5d and 6p Pt electrons, P_d and P_p, were taken as 549×10^{-4} and 402×10^{-4} cm^{-1} (calculated in refs 102 and 103 on the basis of ref 101).

We extended this treatment to the catecholate complex **5**, assuming $5d^8$ configuration of the central atom and that the symmetry of the LUMO of the neutral molecule is not

(100) Benelli, C.; Dei, A.; Gatteschi, D.; Pardi, L. *Inorg. Chem.* **1989**, *28*, 1476.

(101) Rieger, P. H. *J. Magn. Res.* **1997**, *124*, 140.

(102) McInnes, E. J. L.; Farley, R. D.; Macgregor, S. A.; Taylor, K. J.; Yellowlees, L. J.; Rowlands, C. C. *J. Chem. Soc., Faraday Trans.* **1998**, *94*, 2985.

(103) McInnes, E. J. L.; Farley, R. D.; Rowlands, C. C.; Welch, A. J.; Rovatti, L.; Yellowlees, L. J. *J. Chem. Soc., Dalton Trans.* **1999**, 4203.

affected by the replacement of the Cl ligand with the catecholate (b_2 symmetry of π^*-bpy LUMO, C_{2v} point group). The contribution of $5d_{yz}$ and $6p_z$ Pt orbitals in the SOMO of $\mathbf{5}^{-\bullet}$ obtained from the parameters of the EPR spectrum at 77 K was 0.047 and 0.095, respectively. The larger contribution of $6p_z$ orbital and the overall contribution of 14% are consistent with the data reported previously[103] for the SOMO of $[Pt(diimine)Cl_2]^{-\bullet}$. These data, along with the values of g factors, strongly support Pt orbital participation into the SOMO of the radical anion of $\mathbf{5}^{-\bullet}$ and perhaps in the LUMO of the neutral **5**.

Oxidation of **5** yields the radical cation $\mathbf{5}^{+\bullet}$**.** Similar to $\mathbf{5}^{-\bullet}$, a characteristic rhombic EPR spectral profile is observed in the spectrum obtained in the frozen matrix at 77 K (Figure 12). The smaller absolute values of metal hyperfine splitting, A, and the g values obtained for the radical cation $\mathbf{5}^{+\bullet}$ if compared to the radical anion $\mathbf{5}^{-\bullet}$ (Figure 12 caption) suggest smaller contribution of the Pt orbitals into the SOMO of $\mathbf{5}^{+\bullet}$. We attempted to extract the contribution of Pt orbitals into the SOMO of $\mathbf{5}^{+\bullet}$ more quantitatively by extending the treatment described above for the radical anion of Pt(dpphen)(dtbc) to the radical cation $\mathbf{5}^{+\bullet}$. The symmetry of the SOMO in the semiquinone catecholate radical is b_1 if one assumes C_{2v} point group and axes as specified in Figure 12 (*xy* plane is the plane of the molecule; please see ref 104 for the detailed description of the orbitals). Thus, as for $\mathbf{5}^{-\bullet}$, the $5d_{yz}$ and $6p_z$ orbitals are expected to make the most significant contribution of the metal center into the SOMO. This assumption allowed the assignment of the sign for all components of A values for $\mathbf{5}^{+\bullet}$ as opposite to those experimentally determined previously[102,103] for $\mathbf{5}^{-\bullet}$. The hyperfine splitting constants obtained from simulating the EPR spectrum of $\mathbf{5}^{+\bullet}$ (Figure 12, caption) were used to deduce Pt d orbitals contribution in the SOMO of $\mathbf{5}^{+\bullet}$. A $5d^8$ configuration for the metal center in $\mathbf{5}^{+\bullet}$ was assumed since the value of the oxidation potential of **5** and the UV/vis spectrum of $\mathbf{5}^{+\bullet}$ were consistent with the oxidation of neutral **5** being primarily localized on the catecholate ligand. The contribution of $5d_{yz}$ and $6p_z$ Pt d orbitals in the SOMO of $\mathbf{5}^{+\bullet}$ was determined to be -0.045 and -0.027, respectively. This translates to an overall 7% Pt orbital contribution into the delocalization of the SOMO. The positive A values, and consequently "negative" values obtained for electron density on Pt orbitals, reflect the deficiency[105] of the spin density on the Pt nucleus in $\mathbf{5}^{+\bullet}$ if compared to the neutral species.

The sign of the hyperfine splitting constant[105] can be derived on the basis of the expression for $A = (2\mu_0/3)g_e\mu_B\gamma Q$. Here, g_e is the free electron g factor, μ_B is the Bohr magneton, γ is the nucleus magnetogyric ratio which is characteristic for the isotope, and Q is the spin density at the nucleus. For an isotropic EPR spectrum, the sign of A_{iso} is determined by the product of the sign of the nuclear magnetogyric ratio and that of the spin density at the nucleus. Since γ for ^{195}Pt is positive, A_{iso} is expected to be negative if there is an excess of spin density at the Pt center and positive if there is a deficit of electron density on Pt center. For the anisotropic spectrum, the sign of the individual components of A shall be determined individually, and this cannot be done from a conventional EPR spectrum. For the radical cations $[Pt(diimine)Cl_2]^{-\bullet}$, it has been determined previously that A_{xx}, A_{yy}, and A_{zz} are negative. We hence assumed that A_{xx}, A_{yy}, and A_{zz} for $\mathbf{5}^{-\bullet}$ are negative, since a replacement of a Cl ligand by a more donating catecholate in **5** is unlikely to affect the reduction process (see Electrochemical section). As discussed, the metal orbitals involved in redistribution of electron density for the radical cation $\mathbf{5}^{+\bullet}$ are likely to be the same as for the radical anion. Then the signs of A_{xx}, A_{yy}, and A_{zz} for the radical cation will be opposite to that for the radical anion; i.e., A_{xx}, A_{yy}, and A_{zz} for $\mathbf{5}^{+\bullet}$ are assumed to be positive.

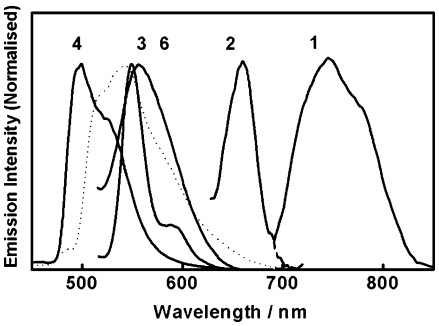

Figure 13. Emission spectra of **1**−**4**, and **6** in tetrahydro-2-methylfuran at 77 K. The spectrum of $Pt(dpphen)Cl_2$ is shown as a dotted line for comparison ($\varphi = 0.07$, emission lifetime = 11 μs).

A smaller contribution of the $6p_z$ orbital in the SOMO of $\mathbf{5}^{+\bullet}$ if compared with the SOMO of $\mathbf{5}^{-\bullet}$ is consistent with the generally accepted localized character of the SOMO in semiquinone radicals bound to the metal center. The participation of metal orbitals in the SOMO of $\mathbf{5}^{+\bullet}$ is very interesting despite the presence of the absorption band at 478 nm in $\mathbf{5}^{+\bullet}$ which matches the energy of the MLCT transition in a valence-localized (3,5-ditertbutyl-semiqunone)-Ni(II) complex. The SOMO in $\mathbf{5}^{+\bullet}$ has a somewhat delocalized character. This result extends to Pt(II) complexes the previous findings on the electronic structure of Re and Mn complexes of 3,5-ditertbutyl-semiqunone.[95] In those studies, the ancillary ligand was shown to tune the extent of electron delocalization within the [M(semiquinone)] chelate ring, leading to a change of metal contribution in the SOMO, which in turn was tuning the energy of the corresponding MLCT transition.

Emission Spectroscopy. Compounds **1**−**4** and **6** are emissive at 77 K in the frozen glass matrix of 2-Me-THF upon excitation into the lowest absorption band (Figure 13). Emission energy is sensitive to the nature of the thiolate or phenolate ligand and increases when the coordination geometry changes from di to bis (e.g., **1** vs **2**) or upon introduction of a more electron-withdrawing thiolate/phenolate ligands (**1** vs **3** or **2** vs **4**). Within the same structural motif, a change from sulfur to oxygen also increases emission energy. No emission was observed for the catecholate complex **5**. In contrast to the other Pt(II)

(104) Gordon, D. J.; Fenske, R. F. *Inorg. Chem.* **1982**, *21*, 2907.
(105) Atherton, N. M. *Principles of Electron Spin Resonance*; Ellis Horwood and PTR Prentice Hall: New York, 1993.

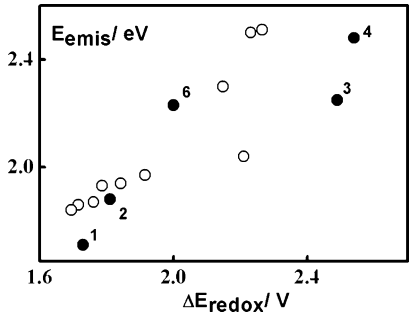

Figure 14. Plot of emission energy at 77 K (E_{emis}) vs the difference between the ground-state oxidation and reduction potentials for the previous diimine dithiolate platinum(II) complexes[1] (○) and complexes **1**−**4** and **6** (●).

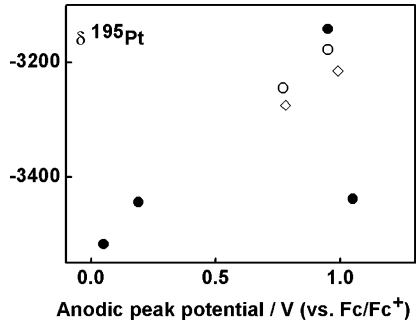

Figure 15. Correlation between anodic peak potential (V, vs Fc/Fc^+) for the thiolates **1**−**4** (●) and for the previously studied Pt(II) diimines with perfluorinated thiolate ligands, featuring bipyridine (○) or phenanthroline (◇). Compound **3**, Pt(dpphen)(dtoc), does not follow this trend.

diimine thiolate/phenolate compounds, the emission spectra for Pt(II) complexes **3** and **4** at 77 K are structured. The 920 cm^{-1} vibrational spacing observed in the emission spectrum of **4** roughly matches the energy of the ν(CS) in **12**. This observation suggests some involvement of intracarborane vibrations in the excitation process and in the process of redistribution of the excitation energy. The emission spectrum of **3** possesses well-defined vibrational progression of about 1350 cm^{-1}, which corresponds to the C═C stretch of the diimine ligand. At 77 K, the quantum yields for Pt(II) chromophores **1, 2**, and **6** are approximately 10^{-3}, whereas the quantum yields for the thiocarborane derivatives **3** and **4** are 100 times larger.

Complexes **3** and **4** are emissive in fluid solution, featuring structureless emission spectrum which is shifted to the lower energies when compared to the spectra at 77 K (Table 3). Emission lifetime of **3** and **4** are 6 and 26 ns, respectively, in aerated CH_2Cl_2 solution at room temperature. Thus, compounds **3** and **4** join the family of relatively rare examples[14,15,22,25] of solution-emitting Pt(II) diimine complexes with donor ligand other than acetylide. One possibility for the enhancement of room-temperature emission is an increase in the energy of the d−d state. Perhaps a strongly electron-withdrawing carborane cage acts as strong-field ligand, making the d−d state less thermally accessible, as with Pt(II) imine acetylides[34,38−55] or cyanides.[56] This observation is also consistent with the higher photostability observed for the carborane derivatives **3** and **4** in comparison to previously known Pt(diimine)(arylthiolates).[65,71] Other factors which might account for carborane complexes being emissive in solution include higher energy of the lowest excited state if compared to the other chromophores studied and vibrational progression observed in the emission spectra which could be indicating smaller intraligand distortion upon excitation for the carborane complexes if compared to their non-carborane counterparts. (We are grateful to the referee for bringing the latter two possibilities to our attention.)

The trend in emission energies of **1**−**4** and **6** follows the trend in absorption energies and the trend established for Pt(diimine)(1,2-dithiolate) complexes (Figure 14) between emission energies and the difference between the oxidation and reduction potentials of the ground state. These data support the picture that the emissive state and the absorbing state are of the same origin, and hence that emission originates from a (charge-transfer-to-diimine) excited state.

Electronic Structure. The nature of the frontier orbitals in **1**−**6** has been determined by a combination of absorption, emission, and (spectro)electrochemical techniques. The charge-transfer nature of the lowest electronic transition is supported by (i) the strong dependence of the absorption energy on the electronic structure of the thiolate or phenolate ligand; (ii) the large solvatochromism; and (iii) the correlation between low-temperature emission energies and the difference between oxidation and reduction potentials of the ground state. The values of the first reduction potential for all the compounds investigated (Table 4) are virtually independent of the donor ligand and are close to the value of the first reduction potential of $Pt(dpphen)Cl_2$, indicating that the LUMO is mostly localized on the π^* orbital of the 4,7-diphenyl-1,10-phenanthroline. This conclusion is further supported by the UV/vis (spectro)electrochemistry results, which show the formation of the diimine-localized absorbencies in the course of the first reversible reduction process. The strong influence of the thiolate/phenolate ligand on the value of the oxidation peak potential and on the absorption energy is indicative of the HOMO being mainly centered on the thiolate/phenolate ligand. For **5**, the EPR spectroscopic data suggest that Pt(II) orbitals participate both in the LUMO and HOMO.

The large increase of the extinction coefficient of the lowest absorption band (from 2250−4000 to 8000−11000 mol^{-1} dm^3 cm^{-1}) upon changing from mono- to bidentate coordination can also be rationalized in terms of increased contribution of Pt orbitals in the HOMO of the latter. Thus, the lowest electronic transition in **1**−**6** studied is charge-transfer from Pt/thiolate(phenolate)-based HOMO to the diimine/Pt-based LUMO.

A correlation is also observed between the ^{195}Pt NMR data and oxidation potentials. The trend in the values of chemical shifts of ^{195}Pt resonances correlates with the trend in the oxidation peak potentials with the thiolate (Figure 15) and phenolate subgroups of complexes. An increase in the anodic peak potential coincides with a less-negative shift in the ^{195}Pt NMR spectrum. Even though there is a rather limited data set available for other thiolate compounds,[2] the data fit this correlation (Table 4, Figure 15). This observation further

supports the conclusion about participation of metal orbitals in the HOMO.

Interestingly, EPR results indicate larger Pt d orbital contribution in the SOMO of the radical anion than the radical cation of **5**. In the neutral species, the situation is likely to be reversed, as evidenced by the large metal center contribution in the HOMO obtained by EH calculations for $Pt(bpy)(PhS)_2$[23] and by a shift in energy of the lowest electronic transition on changing the central atom from Pt(II) to Pd(II). The photophysical properties of Pt(II) thiocarborane compounds, **3** and **4**, differ from those of the other phenolate/thiolate Pt(II) diimine chromophores, despite the same nature of the lowest excited state. Chromophores **3** and **4** exhibit structured emission in fluid solution, which can be rationalized in terms of the strong ligand field of the thiocarboranes, leading to an increase in the energy of the d−d state, thus creating conditions for fluid solution emission of the charge transfer state. For the case of arylthiolate Pt(II) diimine compounds, it has been shown by resonance Raman spectroscopy[71] that none of the intra-thiolate vibrations are significantly affected upon excitation of the MLCT/LLCT band. The pronounced vibrational structure of the emission spectra of **4**, which is different from that observed for $Pt(dpphen)Cl_2$ emission, supports involvement of the orbitals localized on the carborane moiety in the emissive electronic state. Thus, thiocarboranes cannot be considered as direct analogues of arylthiols due to delocalization of HOMO over the carborane cage while in the case of arylthiols the HOMO is more localized on the S atoms.

Conclusion

In the present study, a general route for synthesis of Pt(II) diimine thiolate/phenolates chromophores possessing bulky phenolate or thiolate ligands is reported. The lowest excited state in these new chromophores is assigned to the (charge-transfer-to-diimine) transition from the HOMO of mixed Pt/S (or Pt/O) character. The decrease in energy of the lowest detectable transition on going from bis-mono to di-coordinated donor ligands confirms participation of the donor ligand orbitals in the HOMO and larger Pt d orbital contribution in the HOMO of the complexes with di- vs mono-coordinated donor ligands. The lower extinction coefficient observed for the corresponding transition for the phenolate in comparison to the thiolate chromophores reflects larger mixing of Pt d orbitals with the more donating sulfur atom. Consistent with the energy gap law, the 77 K emission energy decreases along with a decrease in the transition energy, with the lowest emission energy detected for the compound with the most donating and rigid dithiolate ligand. There is a dramatic difference in the photophysical properties of carborane complexes **3** and **4** compared to other mixed-ligand Pt(II) compounds, which includes the presence of room-temperature emission and photostability. Hence, thiocarboranes offer an alternative to the acetylide or cyanide ligands with respect to enabling emission of Pt(II) complexes in solution, which does not require a carbon anion directly bound to the metal center. The reversible oxidation exhibited by Pt(dpphen)(dtbc) allowed for direct probing of the parentage of the HOMO by UV/vis (spectro)electrochemistry and EPR spectroscopy, which confirmed Pt(II) orbital involvement in the HOMO. These results provide additional guidelines and insight to prepare Pt(II) chromophores with specific photophysical properties. Given the broad interest in metal chromophores for applications ranging from electronics to catalysis, continued basic studies to elucidate the underlying chemical/physical phenomena and to create structure−property−function relationships are critical for long-term success.

Experimental Section

Complete details of the synthesis and experiments can be found in the Supporting Information.

Acknowledgment. We thank Duke University and Boston University, Universities of Nottingham and Sheffield, Engineering and Physical Sciences Research Council, and Russian Fund for Basic Research for support, as well as Dr. Celine Taboy for experimental assistance.

Supporting Information Available: Crystallographic data; experimental details. This material is available free of charge via the Internet at http://pubs.acs.org.

IC051733T